Transition-State Structures for *N*-Glycoside Hydrolysis of AMP by Acid and by AMP Nucleosidase in the Presence and Absence of Allosteric Activator†

Frank Mentch,‡ David W. Parkin,§ and Vern L. Schramm*
Department of Biochemistry, Temple University School of Medicine, Philadelphia, Pennsylvania 19140
Received August 4, 1986; Revised Manuscript Received October 6, 1986

ABSTRACT: The mechanism of acid and enzymatic hydrolysis of the N-glycosidic bond of AMP has been investigated by fitting experimentally observed kinetic isotope effects [Parkin, D. W., & Schramm, V. L. (1987) *Biochemistry* (preceding paper in this issue)] to calculated kinetic isotope effects for proposed transition-state structures. The sensitivity of the transition-state calculations was tested by varying the transition-state structure and comparing changes in the calculated kinetic isotope effects with the experimental values of the isotope effect measurements. The kinetic isotope effects for the acid-catalyzed hydrolysis of AMP are best explained by a transition state with considerable oxycarbonium character in the ribose ring, significant bonding remaining to the departing adenine ring, participation of a water nucleophile, and protonation of the adenine ring. A transition-state structure without preassociation of the water nucleophile cannot be eliminated by the data. Enzymatic hydrolysis of the N-glycosidic bond of AMP by AMP nucleosidase from *Azotobacter vinelandii* was analyzed in the absence and presence of MgATP, the allosteric activator that increases V_{max} approximately 200-fold. The transition states for enzyme-catalyzed hydrolysis that best explain the kinetic isotope effects involve early S_N1 transition states with significant bond order in the glycosidic bond and protonation of the adenine base. The enzyme enforces participation of an enzyme-bound water molecule, which has weak bonding to C1′ in the transition state. Activation of AMP nucleosidase by MgATP causes the bond order of the glycosidic bond in the transition state to increase significantly. Hyperconjugation in the ribosyl group is altered by enzymatic stabilization of the oxycarbonium ion. This change is consistent with the interaction of an amino acid on the enzyme. Together, these changes stabilize a carboxonium-like transition-state complex that occurs earlier in the reaction pathway than in the absence of allosteric activator. In addition to the allosteric changes that alter transition-state structure, the presence of other inductive effects that are unobserved by kinetic isotope measurements is also likely to increase the catalytic rate.

Adenosine monophosphate nucleosidase from *Azotobacter vinelandii* catalyzes the reversible hydrolysis of AMP to adenine and ribose 5-phosphate:

$$\text{AMP} + \text{H}_2\text{O} \xrightarrow{\text{MgATP}} \text{adenine} + \text{ribose 5-phosphate}$$

The reaction is activated allosterically by MgATP, which causes an increase in turnover number of approximately 200-fold while causing insignificant changes in the K_m for AMP (Schramm, 1974; DeWolf et al., 1980). The reaction mechanism is concerted, with a rapid-equilibrium addition of AMP and random release of adenine and ribose 5-phosphate (DeWolf et al., 1986). Kinetic isotope effects are consistent with these results and indicate that the observed kinetic isotope effects are intrinsic (Parkin & Schramm, 1984, 1987). An important feature of the kinetic isotope effects is that allosteric activation with MgATP causes disproportionate changes in the individual isotope effects, the pattern expected when allosteric activation alters the structure of the transition state (Parkin & Schramm, 1984, 1987).

The transition-state structure for hydrolysis of AMP involves altered bonds adjacent to the anomeric ribose carbon of AMP (designated C1′ according to the nomenclature shown in Figure 1). To establish the transition-state structure around C1′, it is necessary to measure isotope effects with a minimum of four atoms which are influenced by altered bond structure in the transition state. In the experiments of preceding publications (Parkin et al., 1984; Parkin & Schramm, 1984, 1987), ^{14}C1′, ^{3}H1′, ^{2}H2′ and ^{15}N9 kinetic isotope effects[1] were established for acid-catalyzed hydrolysis and hydrolysis by AMP nucleosidase in the presence and absence of MgATP. These results have permitted qualitative conclusions about the structure of the transition states for these three conditions (Parkin & Schramm, 1984, 1987). Each of the three reaction conditions stabilizes a unique transition-state structure, as indicated by different intrinsic kinetic isotope effects.

The purpose of this work is to establish well-defined transition-state structures for AMP hydrolysis by acid and AMP nucleosidase. Quantitative analysis of transition-state structure for enzyme-catalyzed reactions has been attempted in only a few cases [e.g., Rodgers et al. (1982), Scharschmidt et al. (1984), and Hermes et al. (1984)]. Resolution of the tran-

† This work was supported by Research Grant GM21083 from the National Institutes of Health. Postdoctoral trainee support to D.W.P. was provided by Training Grant AM07163 from the National Institutes of Health for a portion of this research. Preliminary reports of these studies were presented at the meeting of the American Chemical Society, Philadelphia, PA, August 1984.

* Author to whom correspondence should be addressed.
‡ Present address: Department of Chemistry, The Pennsylvania State University, Ogontz Campus, Abington, PA 19001.
§ Present address: Chemistry Department, Chestnut Hill College, Philadelphia, PA 19118.

[1] Heavy atom kinetic isotope effects are abbreviated as follows: ^{14}C1′ represents the V_{max}/K_m kinetic isotope effect of ^{12}C/^{14}C at C1′ of AMP; ^{3}H1′ represents the V_{max}/K_m kinetic isotope effect of ^{1}H/^{3}H at H1′ of AMP; ^{2}H2′ represents the V_{max}/K_m kinetic isotope effect of ^{1}H/^{2}H at H2′ of AMP; and ^{15}N9 represents the V_{max}/K_m kinetic isotope effect of ^{14}N/^{15}N at N9 of AMP. The methods for the determination of the kinetic isotope effects are summarized in Parkin and Schramm (1987).

0006-2960/87/0426-0921$01.50/0

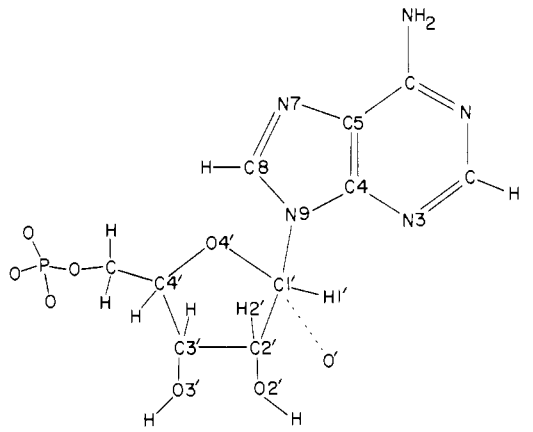

FIGURE 1: Structure of AMP and nomenclature of atoms surrounding the anomeric carbon of ribose 5-phosphate. Only the atoms neighboring C1′ of ribose 5-phosphate and those used in transition-state calculations are labeled. The oxygen labeled O′ is the water nucleophile. AMP is shown in the anti configuration around the glycosyl bond.

sition-state structure requires that isotope effects be measured on enough atoms to report on the nature of the bonds that undergo major changes in the reaction. Glycosidic bond hydrolysis of AMP is well suited to transition-state analysis, since most of the kinetic isotope effects are experimentally accessible, the enzymatic mechanism expresses intrinsic kinetic isotope effects, the magnitude of the isotope effects are sufficient to permit observation of changes induced by the allosteric activator, and a chemical model is available as a benchmark for comparing the enzymatic reactions. Transition-state structures for AMP nucleosidase provide information on the mechanism of enzymatic catalysis and permit the development of a method to determine the effect of allosteric effectors on enzymatic reactions. The results demonstrate the manner in which allosteric activation can alter transition-state structure and therefore increase catalytic efficiency. The systematic variation of transition-state structure in calculations of kinetic isotope effects demonstrates the sensitivity of this method and provides explanations for the observed kinetic isotope effects.

METHODS

Computer Calculations of Transition-State Structures and Kinetic Isotope Effects. The BEBOVIB-IV computer program (bond energy bond order vibrational frequency) (Sims, et al., 1977) was obtained from Indiana University, Quantum Chemistry Program Exchange (Program No. 337). The Fortran program was adapted to run on the CDC Cyber 170-750 computer and the 68000 and 8086 CPU based microprocessors. The NAMOD program (Quantum Chemistry Program Exchange, Program No. 370) was interfaced to the data output of BEBOVIB and permitted graphic presentation of specific structures for reactant state, transition states, or specific vibrational modes. Reactant- and transition-state vibrational energies are approximated by assuming a harmonic potential for each vibrational degree of freedom. Contributions to isotope effects from differences in zero-point energies between the reactant state and the transition state, changes in mass moment of inertia, and changes in populations of excited vibrational states are calculated upon isotopic substitution. Although the BEBOVIB program permits the use of off-diagonal force constants, necessary to accurately reproduce experimental vibrational frequencies, such coupling constants were used only for generation of the reaction coordinate. Vibration frequencies of transition states are not available, and extrapolation of interaction force constants along the reaction coordinate is uncertain. The widespread and successful application of this method is due to the predictable effects of an isotopic substitution. Ratios of reaction rates, as measured in kinetic isotope effect experiments, are more easily calculated than are absolute reaction rates.

Geometry, Force Constants, and the Reaction Coordinate. Bond angles and bond distances for the reactant-state AMP molecule are taken directly from X-ray crystallography results (Kraut & Jensen, 1963) with two exceptions. The bond angles for C1′ in the ribose ring are given standard sp^3 values of 109.5°, and the glycosidic torsion angle O4′–C1′–N9–C8 is taken as 60°. Force constants for bond stretching, angle bending, and torsional angle twisting conform to commonly used values (Fry & Sims, 1974; Wilson et al., 1955). The ground-state models of 15 or 16 atoms include all atoms within two bonds of the reacting C1′–N9 bond. These include the five atoms of the ribose ring and the atoms of the imidazole ring of adenine. This planar component of the adenine ring is "closed" while the ribose ring is "open". The bond between C3′ and C4′ of the ribose ring is omitted in both the reactant-state and the transition-state AMP models. This allows equal-energy ribose configurations for variable bond angles around C1′ without involved ring conformation calculations.

Isotope effects are calculated as a function of transition-state properties. Families of transition states are generated by incremental alterations in one or more structural features. The principal variable is the position along the reaction pathway or reaction coordinate. Progress along the reaction coordinate is measured by the degree of reduction in the C1′–N9 bond order. The hydridization of carbon C1′ changes from sp^3 to sp^2 as the C1′–N9 bond cleaves. If the model includes water nucleophile participation, the geometry of C1′ undergoes inversion when the developing bond order exceeds the bond order to the leaving group. The primary ^{14}C and α-secondary ^3H isotope effects are diagnostic of reaction coordinate position. The β-secondary ^2H isotope effect reports on the degree of hyperconjugation in the transition state relative to the reactant state. This is modeled by increasing the C1′–C2′ bond order while decreasing the C2′–H2′ bond order by the same amount. The primary ^{15}N isotope effect reports on position along the reaction coordinate and bonding changes in the imidazole ring of adenine. Families of transition states were generated that differ in bond orders within the imidazole ring as a function of protonation at N7 and C1′–N9 bond cleavage. Additional families of transition states were generated that varied in N-glycosidic torsion angle or total bond order to C1′.

To calculate the impact of structural variation on isotope effects, these geometry changes were translated into changes in bond distances and stretching and bending force constants. Pauling's rule (eq 1) was used to relate bond distance (r_n) to

$$r_n = r_1 - 0.3 \ln n \quad (1)$$

bond order (n) and single-bond length (r_1). The valence angles at carbon C1′ vary from tetrahedral to trigonal as the C1′–N9 bond order (n_1) decreases and the C1′–O′ bond order (n_2) increases. There is a loss in σ bonding to C1′ if C1′–O′ bond formation lags behind C1′–N9 bond breaking. This may or may not result in π bonding and hyperconjugation (n_3) between atoms C1′ and O4′ and between C1′ and the C2′–H2′ bond. The angle α, N9–C1′–X, for X = H1′, C2′, or O4′, is calculated as a function of n_1, n_2, and n_3 (eq 2). It varies between

$$\alpha = \frac{n_1[90° + (19.5°)n_1] + n_2[90° - (19.5°)n_2] + (90°)n_3}{n_1 + n_2 + n_3} \quad (2)$$

70.5° and 109.5°. The extremes represent sp^3 hybridization

while a value of 90° indicates sp^2 hybridization. Equation 2 reduces to the standard S_N1 formula (eq 3) when $n_2 = n_3 = 0$ and simplifies to the S_N2 equation (eq 4) when $n_3 = 0$ and

$$\alpha = 90° + (19.5°)n_1 \quad (3)$$

$$\alpha = 70.5° + (39°)n_1 \quad (4)$$

$n_1 + n_2 = 1$. Stretching force constants vary linearly with bond order (eq 5). Stretching force constants for the bonds C1′–O4′, C1′–C2′, and C1′–H1′, which undergo considerable change in hybridization, are calculated from eq 6, in which

$$f_n = nf_1 \quad (5)$$

$$f_{n,\alpha} = nf_{1,109.5°}[1 + S[1 - (\alpha - 90°)/19.5°]] \quad \text{for } \alpha > 90° \quad (6)$$

S, the fractional difference between sp^2 and sp^3 force constants, is taken as 0.11 for oxygen and carbon and 0.04 for hydrogen. Bending force constants vary with bond orders n and m and with angle θ by eq 7 for a concerted S_N2 reaction coordinate and by eq 8 for all other reaction coordinates. Equation 9 defines g as a function of the bond angle θ. Torsional force constants are held constant.

$$f_{n,m,\theta} = g_\theta nmf_{1,1,109.5°} \quad (7)$$

$$f_{n,m,\theta} = g_\theta n^{1/2}m^{1/2}f_{1,1,109.5°} \quad (8)$$

$$g_\theta = 1.39 + 1.17 \cos\theta \quad (9)$$

The reaction coordinate motion used for the S_N1 transition state is generated by making the C1′–N9 stretching force constant equal to a small negative number, typically −0.2 mdyn/Å. For those transition states with partial C1′–O′ bond formation, the reaction coordinate is the asymmetric O′–C1′–N9 stretch generated by adding an interaction force constant f_{ij} to couple the O′–C1′ and C1′–N9 stretches:

$$f_{ij} = 1.1(f_if_j)^{1/2} \quad (10)$$

More complex reaction coordinates that weakly couple valence angle bends to the two previous coordinates were also examined. With the exceptions of eq 2–4 and 6, the force constant, bond order, and bond angle relationships are incorporated in the BEBOVIB-IV program and are discussed in Sims & Lewis (1984).

Results

Calculated Kinetic Isotope Effects. The kinetic isotope effects expected for S_N1-like and S_N2-like transition states in AMP glycosidic bond hydrolysis were calculated as a function of the development of the transition state at different points along the reaction coordinate (Figure 2). The calculated kinetic isotope effects are compared to the experimental kinetic isotope effects determined for acid-catalyzed hydrolysis and hydrolysis catalyzed by AMP nucleosidase both in the absence and in the presence of allosteric activator. The results of this comparison indicate that the ^{3}H1′, ^{2}H2′, and ^{14}C1′ kinetic isotope effects for acid-catalyzed hydrolysis of AMP agree with isotope effects calculated for an S_N1-like transition state. However, the ^{15}N9 isotope effect is less than expected for a transition state with classic S_N1 character, i.e., with fully developed carbocation character. This difference can be corrected by protonation of N7 in the reactant molecule (see below). The experimental kinetic isotope effects for the enzyme-catalyzed reaction agree less well with the isotope effects calculated for an S_N1 intermediate when the ^{3}H1′ isotope effects are aligned with the calculated isotope effects. Likewise, alignment of the ^{2}H2′ isotope effects causes large disagreements of the other isotope effects. Although the acid-catalyzed hydrolysis approximates an S_N1-like transition state, the enzyme-catalyzed hydrolysis conforms less well. Neither acid- nor enzyme-catalyzed reactions conform to S_N2-like structures (Figure 2B) since isotope effects differ considerably from those expected for S_N2 displacement of adenine.

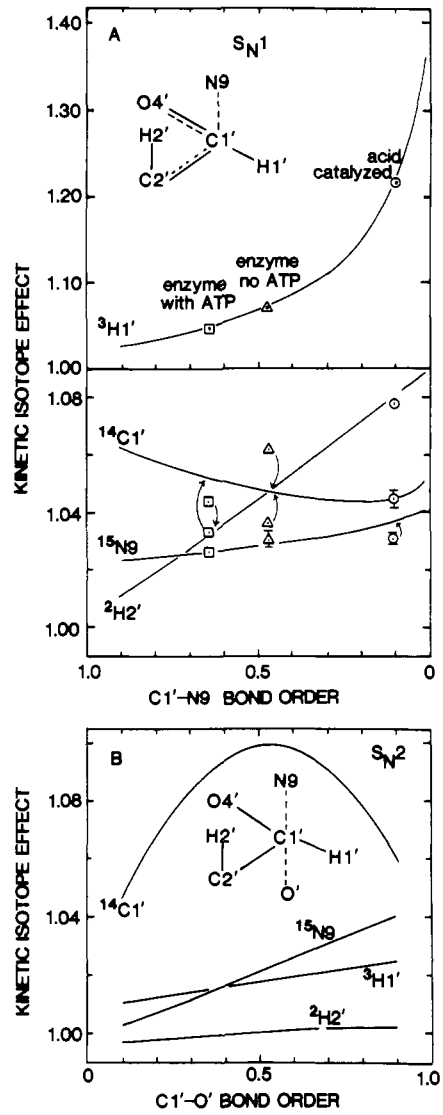

FIGURE 2: Comparison of predicted and observed kinetic isotope effects for classic S_N1 and S_N2 transition states of AMP *N*-glycoside bond hydrolysis. Panel A presents the calculated kinetic isotope effects (solid lines) for classic S_N1-like transition states as a function of the C1′–N9 bond order in the transition state (abscissa). The adenine ring was assumed to be unprotonated in the reactant AMP and the transition state. A C1′–N9 bond order of 0 on the abscissa represents a fully developed carboxonium ion in the transition state with no preassociated water nucleophile. Force constants of individual bonds were changed as a function of bond order and hybridization as described under Methods. The increase of bond order in the C1′–C2′ bond was assigned by the expression $\Delta n_{C1'-C2'} = (1 - n_{C1'-N9} - n_{C1'-O'})/18$, where n represents bond order of the subscripted bond. The data points in panel A represent the experimental kinetic isotope effects for the acid (circles) and AMP nucleosidase catalyzed reactions with (squares) and without (triangles) allosteric activation. The experimental data in the upper panel were aligned with the calculated ^{3}H1′ kinetic isotope effects, and the experimental data for the ^{14}C1′, ^{15}N9, and ^{2}H2′ kinetic isotope effects are aligned with the same transition-state structure in the lower panel of A. The arrows indicate the extent of disagreement between calculated and experimental data for each of the isotope effects. Panel B presents the calculated kinetic isotope effects for an S_N2 transition state with no carbocation development ($n_{C1'-O'} + n_{C1'-N9} = 1$). The experimentally determined isotope effects were widely divergent from the calculated values in panel B and are not shown.

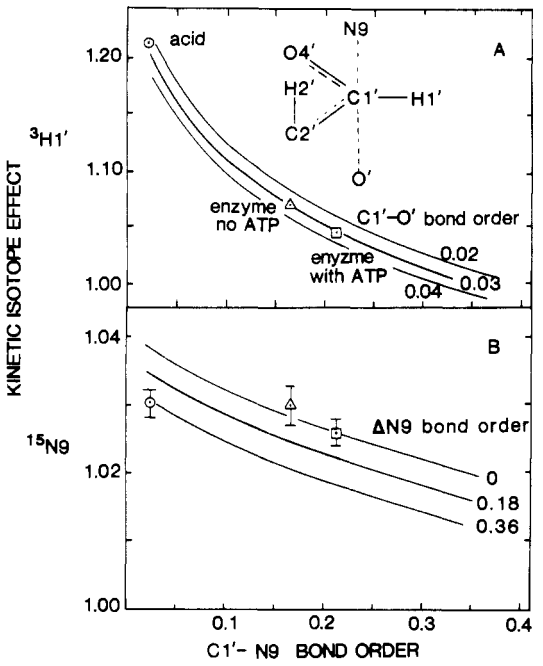

FIGURE 3: Comparison of calculated and observed kinetic isotope effects for a hybrid reaction mechanism as a function of C1′–N9 bond order in the transition state for *N*-glycoside bond hydrolysis of AMP. The solid lines are the calculated ^{3}H1′ and ^{15}N9 kinetic isotope effects in the upper and lower panels, respectively. The calculated kinetic isotope effects assumed that the sum of the bond order to C1′ was 4.0 for all transition states. Bending force constants were varied with the transition-state geometry in an S_N1-like change, and the adenine ring was rotated to give a *syn*-glycosyl torsion angle in the transition state. Changes in the glycosyl torsion angle have no significant influence on the magnitude of the kinetic isotope effects (see Results). The parameters for the AMP reactant structure were taken from the X-ray crystal structure of AMP (see Methods). In panel A, the influence of changing C1′–O′ and C1′–N9 bond order on the calculated ^{3}H1′ isotope effects is superimposed on the experimental isotope effects. In panel B, the effect of change in bond order for C1′–N9 and the effect of change in the imidazole ring bond order to N9 in the transition state are superimposed on the experimental isotope effects. The C1′–O′ bond order in panel B was fixed at 0.03.

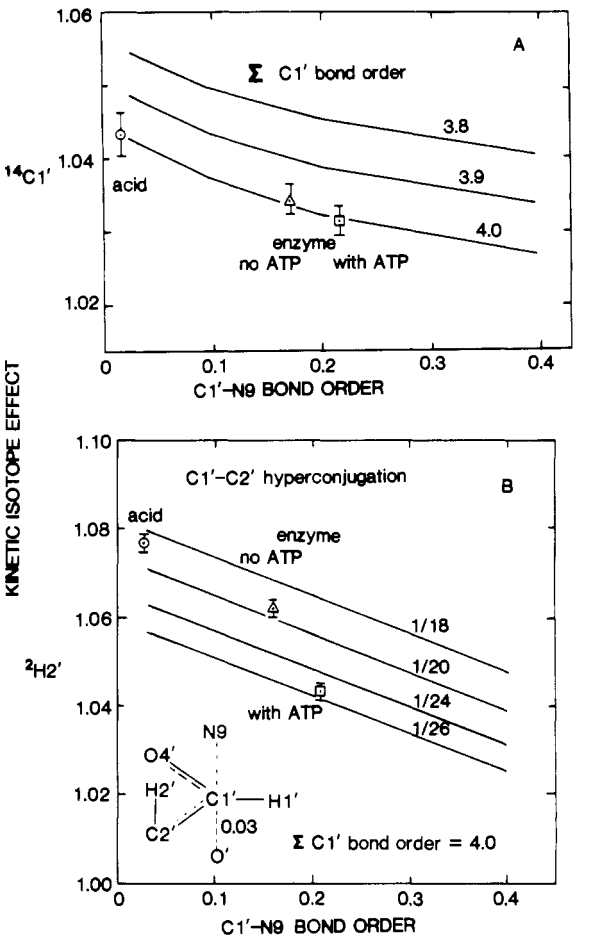

FIGURE 4: Effect of changing C1′–N9 bond order on the calculated kinetic isotope effects for *N*-glycoside bond hydrolysis of AMP. The transition-state structure was similar to that for the calculations in Figure 3. The bond order of C1′–O′ = 0.03, the glycosyl torsion angle of the transition state is opposite that of the reactant state, and the force constants change with bond hybridization similar to an S_N1-like transition state. These factors are described in more detail under Methods. Panel A demonstrates the sensitivity of the ^{14}C1′ kinetic isotope effect to C1′–N9 bond order and total bond order to C1′. The lines are calculated from the BEBOVIB program, and the data points are the experimentally determined values for ^{14}C1′. Panel B demonstrates the sensitivity of the ^{2}H2′ kinetic isotope effects to changes in C1′–N9 bond order and to the fraction of carbocation stabilization attributed to C1′–C2′ hyperconjugation. The points are placed to correspond to the C1′–N9 bond orders defined by the experimental points in Figure 3 and panel A.

Calculated Kinetic Isotope Effects for Hybrid Mechanisms. Transition-state structures that are consistent with the measured kinetic isotope effects were established by varying the transition-state structures for (1) the degree of association of an oxygen nucleophile with the anomeric carbon (C1′) of ribose 5-phosphate, (2) the bond orders to atoms of AMP bonded to C1′, and (3) protonation and geometry of adenine in the reactant and/or transition states to obtain agreement between the observed and calculated families of isotope effects. The calculated isotope effects for the acid-catalyzed reaction were consistent with an S_N1-like transition state while the enzymatic reaction was consistent with hybrid intermediates with significant bond order remaining in C1′–N9 or developing in C1′–O′. The experimentally determined kinetic isotope effects for acid- and enzyme-catalyzed reactions are compared to the calculated transition states in Figures 3 and 4. Each panel illustrates the sensitivity of calculated isotope effects to two parameters of transition-state structure. The major variable for all calculations was the C1′–N9 bond order in the transition state, which forms the abscissa of the plots and indicates the sensitivity of isotope effects to position of the transition state along the reaction coordinate. The second variable demonstrates the sensitivity to other parameters of transition-state structure.

Initial calculations similar to those of Figure 2 demonstrated that only S_N1-like transition states with restricted out-of-plane motion of H1′ could account for the observed kinetic isotope effects for the enzymatic reaction. Each panel compares the acid-catalyzed reaction, which is established to have S_N1 characteristics with C1′–N9 bond order near 0, to the reactions catalyzed by AMP nucleosidase in the absence or presence of MgATP.

Effect of C1′–O′ Bond Order on Calculated Isotope Effects. The experimental isotope effects gave good agreement with a transition-state structure with C1′–O′ bond order near 0.03 (Figure 3A). This conclusion was based on a family of curves similar to those in Figure 3A but which compared ^{15}N9 and ^{14}C1′ isotope effects. For each catalyst (i.e., acid; enzyme, no ATP; enzyme with ATP) only two transition structures were consistent with experimental isotope effects. One transition state for acid had a C1′–N9 bond order of 0.02 and a C1′–O′ bond order of 0.02. The second has no C1′–O′ bond in the transition state but has an increased C1′–N9 bond order. This mechanism is discussed below. One set of transition-state structures for the enzyme with no ATP had a C1′–N9 bond

order of 0.16 and a C1′–O′ bond order of 0.03. A similar fit was obtained for transition states with reversed bond orders, i.e., 0.17 bond order in C1′–O′ and 0.03 in C1′–N9 (results not shown). With ATP, one enzymatic transition state had a C1′–N9 bond order of 0.21 and a C1′–O′ bond order of 0.03. Similar fits of the data were accomplished with reversed bond orders of 0.21 for C1′–O′ and 0.03 for C1′–N9. Variation of the bond orders by more than 0.01 causes disagreement between the theoretical and experimental results for any of these structures.

Effect of N9 Bond Order on Calculated Isotope Effects. Protonation of N7 of the adenine ring alters the bond order in the imidazole ring to N9 both in the reactant AMP and in the transition state. This effect was included in the calculations by varying the difference in bond order to N9 in the reactant and transition states. These calculated isotope effects for AMP hydrolysis by acid and AMP nucleosidase are compared to the experimental kinetic isotope effects in Figure 3B. The calculated ^{15}N9 isotope effect varies by 1% as bond order to N9 is increased by 0.36 in the transition state, the estimated value resulting from loss of the N9–C1′ bond in an S_N1-like transition state (see Discussion). Acid-catalyzed hydrolysis is most consistent with a low C1′–N9 bond order in the transition state while the preferred enzymatic transition states (see Discussion) correspond to C1′–N9 bond orders of 0.16 and 0.21 in the absence and presence of allosteric activator. The bond orders for C1′–N9 are constrained by the values of the other isotope effects; however, the major influence of N9 bond order in the transition state is on the ^{15}N9 isotope effect.

Effect of Total Bond Order to C1′ on Calculated Kinetic Isotope Effects. Kinetic isotope effects most sensitive to the total bond order to C1′ in the transition state are those from ^{14}C1′ (Figure 4A) and ^{3}H1′ (not shown). Variation of total bond order from 3.8 to 4.0 gave changes in the calculated ^{14}C1′ and ^{3}H1′ kinetic isotope effects that would be significant at 0.05 bond order relative to the uncertainty of the measured kinetic isotope effects. Alignment of the ^{14}C1′ and ^{3}H1′ kinetic isotope effects along a constant C1′–N9 bond order is only possible at a total C1′ bond order of 4.0 for the three catalytic reactions. For example, moving the ^{14}C1′ kinetic isotope value for "enzyme, no ATP" to a total C1′ bond order of 3.9 moves the C1′–N9 bond order to a value near 0.6, clearly inconsistent with the calculations in Figures 3 and with an S_N1-like transition state.

The family of calculations analogous to those in Figure 4A were also completed for the ^{3}H1′, ^{15}N9, and ^{2}H2′ kinetic isotope effects. The ^{15}N9 and ^{2}H2′ isotope effects are relatively insensitive to the total bond order to C1′. The ^{3}H1′ isotope effects gave a family of lines similar to those of Figure 3A where the calculated kinetic isotope effect increases as the total bond order to C1′ decreases. As in Figure 4B, the data were consistent with a total bond order of 4.0 to C1′ in the transition state. For calculations of the remaining isotope effects the total bond order to C1′ was fixed at 4.0.

Effect of Hyperconjugation on Calculated ^{2}H2′ Kinetic Isotope Effects. The ^{2}H2′ kinetic isotope effect arises from the increased C1′–C2′ bond order and decreased C2′–H2′ bond order in the furanose ring in the transition state, which in turn causes an alteration in the vibrational frequency of H2′ (see Methods). The magnitude of the ^{2}H2′ isotope effect is therefore not strongly influenced by small changes in C1′–O′ bond order or the total bond order to C1′. The linear change in the ^{2}H2′ isotope effect as a function of C1′–N9 bond order seen in Figure 4B is a result of decreasing O4′–C1′ and C1′–C2′ bond orders as C1′–N9 increases. The larger ^{2}H2′ kinetic isotope effect with larger fractions of "C1′–C2′ hyperconjugation" is a consequence of increasing the importance of hyperconjugation in carbocation stabilization. The ^{2}H2′ isotope effect at constant C1′–N9 bond order increases as the fraction of hyperconjugation in C1′–C2′ increases. A larger fraction of hyperconjugation implies an increased C1′–C2′ bond order and a decreased C1′–O4′ bond order. The value of $^{1}/_{18}$ in Figure 4B corresponds to a C1′–C2′ bond order of unity *plus* $^{1}/_{18}$th of the excess bond order[2] in the ribose ring. The C1′–O4′ bond order is unity plus $^{17}/_{18}$th of the excess bond order.

Table I: Effect of Changing Force Constants on Calculated Kinetic Isotope Effects[a] for *N*-Glycoside Bond Hydrolysis of AMP

force constants	calcd kinetic isotope effect		
	^{14}C1′	^{3}H1′	^{15}N9′
reference values[b]	1.0302	1.0495	1.0266
change in C1′–N9 force constant			
5%	1.0318	1.0495	1.0271
10%	1.0334	1.0495	1.0276
change in C1′–C2′ force constant			
5%	1.0303	1.0494	1.0266
10%	1.0303	1.0493	1.0266
change in H1′–C1′–C2′ bending force constant			
5%	1.0303	1.0529	1.0266
10%	1.0304	1.0563	1.0266

[a] The transition-state structure assumed S_N1 bending force constants, C1′–N9 bond order of 0.21, C1′–O′ bond order of 0.03, and opposite glycosidic torsion angles in reactant and transition states. Other features of the transition state are given under Methods or in reference to structure labeled "Transition State, with ATP" from Figure 5. [b] Reference values for force constants are described under Methods.

Acid-catalyzed hydrolysis and enzyme-catalyzed (no ATP) hydrolysis of AMP cause approximately $^{1}/_{19}$th of furanose hyperconjugation to reside in C1′–C2′, while the enzyme-catalyzed reaction with ATP stabilizes a transition state with only $^{1}/_{26}$th of hyperconjugation at C1′–C2′. Since the ^{2}H2′ isotope effects are relatively independent of the other variables in the transition state, the experimental points are positioned at C1′–N9 bond orders determined from the isotope effect results presented above.

Sensitivity of Calculated Kinetic Isotope Effects to Changes in the Base Values of Force Constants. The key force constants for isotope effect calculations are those that define bonding to isotopically substituted atoms. Differences in the values of key force constants between reactant and transition state largely determine the magnitude of calculated kinetic isotope effects. As eq 5–8 show, the changes in force constants with structure are calculated relative to a base value. For stretching force constants the base value is the force constant of a single bond. The base value for bending force constants is the force constant of a tetrahedral angle subtended by two bonds of unit bond order. Changes in base values affect the absolute magnitude but not the relative magnitude of force constant differences between reactant and transition state. Table I shows calculated isotope effects as a function of 5% and 10% increases in the base values of several key force constants. The α-^{3}H isotope effect shows the greatest sensitivity to base value changes, increasing by 0.007 with a 10% change in the H1′–C1′–C2′ bending force constant. A 10% increase on the C1′–N9 stretching force constant base value

[2] Excess bond order refers to the increase in C1′–O4′ and C1′–C2′ bond orders above unity needed to compensate for the decrease in the sum of C1′–O′ and C1′–N9 bond orders below unity.

Table II: Comparison of Experimental[a] and Calculated[b] Kinetic Isotope Effects for the Transition States of Figure 5

	acid catalyzed[c]			enzyme, no ATP		enzyme with ATP	
isotope effect	exptl	O′ participation	no O′ participation	exptl	calcd	exptl	calcd
^{14}C1′	1.044 ± 0.003	1.044	1.044	1.035 ± 0.002	1.034	1.032 ± 0.002	1.030
^{3}H1′	1.216 ± 0.004	1.218	1.213	1.069 ± 0.002	1.073	1.047 ± 0.002	1.049
^{15}N9	1.030 ± 0.002	1.031	1.029	1.030 ± 0.002	1.029	1.025 ± 0.002	1.027
^{2}H2′	1.077 ± 0.002	1.078	1.079	1.061 ± 0.002	1.062	1.043 ± 0.002	1.046

[a] Experimentally determined kinetic isotope effects are from Parkin and Schramm (1987). [b] Kinetic isotope effects are expressed as the V_{max}/K_m ratio for the light isotope divided by the V_{max}/K_m ratio for the heavy isotope. [c] The calculated kinetic isotope effects for the acid-catalyzed reaction were obtained for an S_N1 transition state without nucleophile preassociation as described under Discussion *or* for the acid-catalyzed transition state with preassociation as shown in Figure 5. The bond orders for the transition-state structures are given in the text.

increases the ^{14}C effect by 0.003 and the ^{15}N effect by 0.001. These changes show that significant changes in force constant base values have a minimal effect on calculated kinetic isotope effects.

Effect of Protonation of O′ on Calculated Kinetic Isotope Effects. Calculated kinetic isotope effects used an oxygen atom as the nucleophile as illustrated in Figure 1. Acid-catalyzed solvolysis (pH <2) is likely to involve a water molecule as the nucleophile, while enzyme-catalyzed hydrolysis is more likely to involve an enzyme-bound water or a hydroxyl ion. The effect of protonation on the calculated kinetic isotope effects was evaluated by using water as the nucleophile. Kinetic isotope effects were calculated for ^{3}H1′, ^{2}H2′, ^{14}C1′, and ^{15}N9 by using the BEBOVIB program. The isotope effects for transition-state structures similar to those described in Figure 3 were affected by less than 0.003, the confidence limits of the measurements. Thus, these calculated isotope effects are not sensitive to the use of O′ or H_2O' as the nucleophile.

Effect of Conformational Changes. Rotation of adenine with respect to the glycosyl torsion angle in the transition state had no significant effect on the calculated kinetic isotope effects. For example, transition-state structures with equal or opposite (180°) glycosyl torsion angles gave nearly identical calculated kinetic isotope effects.

Discussion

The purpose of this study was to establish the transition-state structures for the acid and AMP nucleosidase catalyzed hydrolysis of the N-glycosidic bond of AMP. Enzyme-catalyzed hydrolysis of AMP has the potential for expressing different transition states, since MgATP, the allosteric activator, causes approximately a 200-fold increase in the turnover number with no change in K_m (Schramm, 1974). The preceding paper (Parkin & Schramm, 1987) demonstrated that AMP nucleosidase expresses intrinsic kinetic isotope effects in a concerted reaction mechanism, permitting the transition-state structure to be solved. This discussion compares the transition-state structures for the chemical and enzymatic mechanisms of glycosidic bond hydrolysis.

Acid-Catalyzed Hydrolysis of AMP. Chemical and partial isotope effect studies of inosine, adenosine, and AMP hydrolysis by acid have established that the reaction is S_N1-like with diprotonated adenine as the leaving group (Garrett & Mehta, 1972; Romero et al., 1978; Parkin et al., 1984). This result was confirmed by the more complete kinetic isotope effects reported by Parkin and Schramm (1987). An issue that remains unresolved for the *N*-glycoside hydrolysis of AMP is the degree of oxycarbonium ion development in the transition state. Jencks (1980) has argued that the lifetime of a fully developed oxycarbonium ion in water is too short for significant diffusion and concludes that such mechanisms involve preassociation with solvent nucleophiles. The results of this study indicate incomplete carboxonium formation since a fully developed carboxonium would be expected to give a ^{3}H1′ isotope effect near 1.40 (Melander & Saunders, 1980; see also Figure 2A) while the observed effect is 1.216. Good agreement of the data to an S_N1-like transition state without nucleophilic preassociation was obtained for a transition state with the bond orders C1′–N9 = 0.10, C1′–O4′ = 1.85, C1′–C2′ = 1.05, C2′–H2′ = 0.95, total bond order to C1′ = 4.0, and increased imidazole bond order to N9 of 0.36, consistent with N7 protonation in reactant and transition states. A comparison of the experimental and calculated isotope effects is given in Table II.

The experimental kinetic isotope effects for acid-catalyzed hydrolysis can also be modeled with a transition state that involves the preassociation of a water molecule. This transition state is illustrated in Figure 5. The structure labeled "Transition State, acid" in Figure 5 requires weak nucleophilic preassociation from water (O′), a low bond order to the leaving adenine, and protonation of N7 in the reactant- *and* transition-state structures, with an increase in the imidazole bond order to N9 by 0.36 in the transition state. This transition state has considerable oxycarbonium character, with a C1′–C2′ bond order of 1.054 and a C1′–O4′ bond order of 1.91. Thus the C1′–C2′ bond has 5.6% of the excess bond order in the ribose 5-phosphate ring. The nearly linear response of the ^{2}H2′ kinetic isotope effect to C1′–C2′ bond order provides a convenient method for discriminating S_N1- and S_N2-like transition states, since the ^{2}H2′ kinetic isotope effect is 1.000 ± 0.003 for an S_N2-like transition state with no carbocation formation (Figure 2B). The O′–C1′–N9 valence angle was assumed to be linear, and the geometry of adenine with respect to ribose 5-phosphate was assumed to have the same glycosyl torsion angle as the reactant structure of AMP (compare structure labeled "Reactant State AMP" in Figure 5).

The transition-state model for acid hydrolysis of AMP in Figure 5 is sensitive to small changes in bond order. Thus, changes in any of the indicated bond orders by greater than ±0.01 caused one or more of the calculated kinetic isotope effects to be outside the range of the experimental measurements. Nevertheless, the proposed acid transition state of Figure 5 cannot be distinguished from the S_N1-like transition state discussed above on the basis of the isotope effects. However, the S_N1 transition state requires a glycosidic bond order of 0.10 and prohibits participation of a solvent nucleophile. Since solvent may participate (Jencks, 1980), the acid-catalyzed transition state shown in Figure 5 is preferred.

Enzyme-Catalyzed Hydrolysis of AMP without Allosteric Activator. The transition state for the enzyme without ATP activation has S_N1 character, indicated by the large ^{2}H2′ isotope effect, but is clearly different from either classic S_N1- or S_N2-like transition states (Figure 2). The transition-state structure shown in Figure 5 corresponds to the kinetic isotope

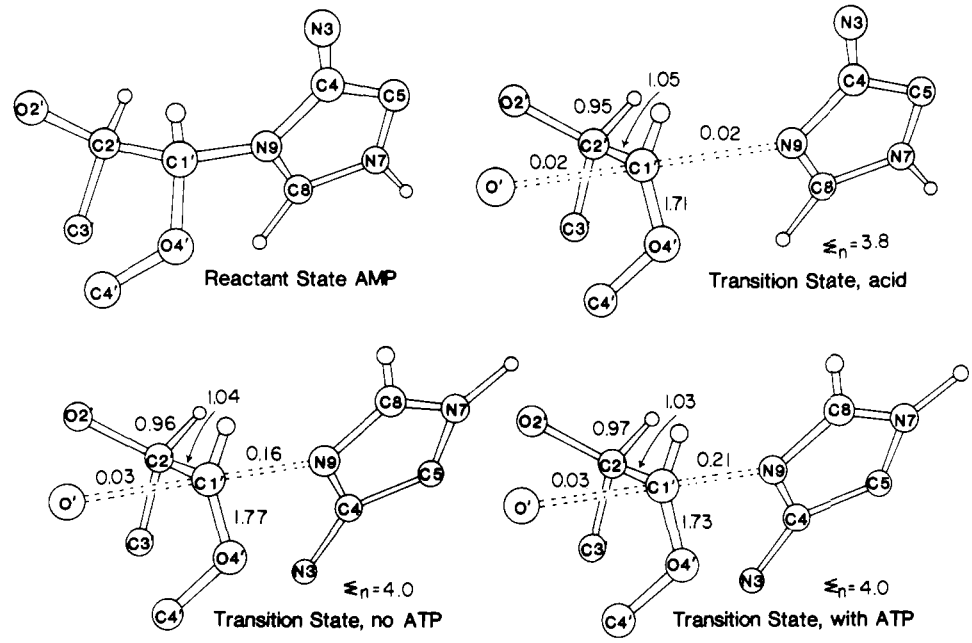

FIGURE 5: Reactant- and transition-state structures for acid and AMP nucleosidase catalyzed hydrolysis of AMP. The structure labeled "Reactant State AMP" is the conformation of AMP taken from the X-ray crystal structure with the glycosyl torsion angle in the anti configuration. Only the atoms used in calculating the kinetic isotope effects are shown. Unlabeled atoms are hydrogen. Bond orders α to C1′ are not given in the reactant state but are set at 1.00. Bond orders for N9–C8 and C8–N7 are 1.37 and 1.73, respectively, in adenine with protonated N7. The structure labeled "Transition State, acid" is a calculated transition state that agrees with the experimental kinetic isotope effects for acid-catalyzed hydrolysis of AMP. The values adjacent to the bonds represent the bond order in the transition state. The changes in bond order as a function of structural changes are detailed under Methods. Note that adenine has the same glycosyl torsion angle (rotation of adenine around the C1′–N9 bond) as in the reactant molecule. The O′ is the oxygen nucleophile of H_2O. The structure labeled "Transition State, no ATP" is a calculated transition state that agrees with the experimental kinetic isotope effects for AMP nucleosidase in the absence of ATP. Note that the adenine ring has been rotated 180° around the C1′–N9 bond to the syn configuration. The structure labeled "Transition State, with ATP" is the calculated transition state that agrees with the experimental kinetic isotope effects for AMP nucleosidase in the presence of ATP. Reactant-state AMP for the enzyme-catalyzed reaction is the same as the structure labeled "Reactant State AMP" except that N7 is unprotonated. (See Figure 7 for AMP in the reactant state for enzymatic catalysis.) The $\sum_n = 4.0$ refers to the sum of bond order to C1′ in the transition-state structure.

effects measured for the enzyme under these conditions. The experimental and calculated kinetic isotope effects for this transition state are summarized in Table II. Since the isotope effects are V_{max}/K_m effects, free AMP at pH 8.0 is the reactant state. Under these conditions, N7 will not be protonated.

The major difference between the acid-catalyzed and enzyme-catalyzed reactions is the C1′–N9 bond order. In the acid-catalyzed transition state, the glycosidic bond is nearly cleaved, while in the enzyme-catalyzed reaction, bond order to the departing adenine increases to 0.16. The large decrease in the ^{3}H1′ isotope effect (1.216 to 1.069) from acid- to enzyme-catalyzed reaction reflects the restriction on out-of-plane H1′ bending imposed by the bonds to N9 and the oxygen nucleophile. The relatively small change in the ^{2}H2′ isotope effect from acid-catalyzed hydrolysis (from 1.077 to 1.061) demonstrates nearly unchanged hyperconjugation in the ribose ring and establishes the oxycarbonium character. Participation of an enzyme-directed water nucleophile in the transition state is indicated from the inability of solvent nucleophiles to replace H_2O (DeWolf et al., 1986).

The ^{15}N9 isotope effect of 1.030 for the enzyme is the same as for acid-catalyzed hydrolysis (Table II). However, protonation of reactant-state AMP differs for these conditions. Protonation of N7 of AMP makes adenine a better leaving group, the proposed basis for acid-catalyzed hydrolysis. It was therefore assumed that N7 is protonated in both the reactant and transition states for the acid-catalyzed reaction (pH <2) (see Figure 5). At pH 8, the AMP substrate is not significantly protonated (pK_a of N7 is ~1). However, enzymatic catalysis is likely to involve protonation of N7 since tubercidin 5-phosphate (7-deaza-AMP) is not a substrate (DeWolf et al., 1979). Transition-state resonance structures of the imidazole ring of adenine suggest that, for a nearly cleaved C1′–N9 bond, the N7 protonated leaving group (a) will have a higher bond order to N9 than does the nonprotonated leaving group (b).

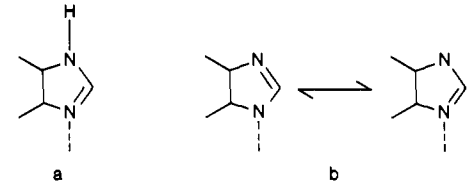

a b

This results in a lower ^{15}N isotope effect for the protonated pathway. The presumed increase in bond order to N9 within the imidazole ring from leaving group a is 0.36 as indicated in Figure 3B, while for the average of the resonance structures in b, the estimated increase in bond order to N9 would be 0.18 (Figure 3B). A C1′–N9 bond order of 0.16 proposed for the transition state with no ATP (Figure 5) adds additional bond order to N9. The ^{15}N9 isotope effect of 1.030 for enzyme without activator indicates that the imidazole contribution to N9 bond order is approximately equal in the reactant and transition states, while protonation of N7 is implicated by the lack of catalytic activity for tubercidin 5-phosphate (DeWolf et al., 1979). The reactant- and transition-state structures:

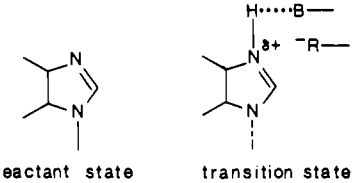

are consistent with these isotope effects, where an acid at the catalytic site protonates N7 and a base stabilizes the excess

bond order of the imidazole near N7. Thus, the transition state is shown with protonation of N7.

Another feature of the enzymatic transition state is that adenine is rotated 180° with respect to reactant AMP. Rotation of adenine around the glycosyl bond (alteration of the glycosyl torsion angle) has no effect on the calculated kinetic isotope effects. However, from the finding that nucleotide analogues with *syn*-glycosyl torsion angles bind strongly to AMP nucleosidase (DeWolf et al., 1979), the configuration of AMP is assumed to be syn in the transition state.

The fraction of hyperconjugation residing in C1′–C2′ for the enzymatic reaction is similar to that for the acid-catalyzed reaction (Figure 4B). Enzymatic stabilization of the oxycarbonium would alter this distribution as is seen for the enzymatic reaction with ATP (see below).

Enzyme-Catalyzed Hydrolysis of AMP with Allosteric Activator. Allosteric activation caused a relatively large decrease in the ^{3}H1′ and ^{2}H2′ isotope effects with much smaller changes in the ^{14}C1′ and ^{15}N9 isotope effects (Table II). The transition state that best corresponds to this reaction is given in Figure 5. Differences caused by MgATP activation are primarily an increase in C1′–N9 bond order from 0.16 to 0.21 and a decrease in the fraction of the hyperconjugation in the ribose ring that resides at C1′–C2′. Part of the change in C1′–C2′ bond order is due to the increase in C1′–N9 bonding, which decreases the positive charge (excess bond order) in the ribose ring. However, for the acid-catalyzed reaction and enzyme without ATP, approximately $^{1}/_{19}$th of the excess bond order resides in C1′–C2′ while this decreases to approximately $^{1}/_{26}$th of the excess as a consequence of allosteric activation (Figure 3B). This parameter is readily quantitated by the ^{2}H2′ β-secondary isotope effect and represents a significant change in transition-state structure. Stabilization of the oxycarbonium charge by a catalytic site anion would account for this effect. An alternative explanation involves a change in the angle between the C2′–H2′ bond with respect to the C1′–N9 bond. The magnitude of the ^{2}H2′ effect is greatest when these bonds are eclipsed (Sunko et al., 1977). Models of the transition-state structure with C1′ nearly trigonal planar indicate that these bonds are within 5° of eclipse and changes of ±15° from this position require considerable distortion of the ribose ring. A change of 30° would be required to account for the change in the ^{2}H2′ isotope effect that results from the addition of allosteric activator. Thus, alteration in hyperconjugation is considered the more likely explanation for the altered β-isotope effect.

The V_{max}/K_m vs. pH profile for AMP nucleosidase in the presence of MgATP identified two groups with pK_a values near 6.6 which must be unprotonated for activity and two groups with pK_a values near 8.2 which must be protonated for activity (DeWolf et al., 1979, 1986). One group at pK_a = 6.6 is likely to be the phosphate of AMP, leaving three ionizable groups in the experimental range of pH 6–9.5. The proposed transition state for AMP nucleosidase can accommodate these groups as indicated in Figure 6. In the transition state the substrate has the syn configuration, which is anchored by binding of the phosphate (pK_a ~ 6.6) to one of the groups ($^{+}$HR$_3$) with a pK_a near 8.2. Also participating, but not shown in Figure 6, are hydrogen bonds to the 2′- and 3′-hydroxyls since V_{max}/K_m values for deoxy-AMP's are approximately 40-fold lower than for AMP (DeWolf et al., 1979). The enzyme-bound water nucleophile requires ionization for attack on C1′, and this is a likely role for the second group with a pK_a near 6.6 in the V_{max}/K_m profile. The fourth group in the pH profile is R_4, which protonates N7 in the transition state

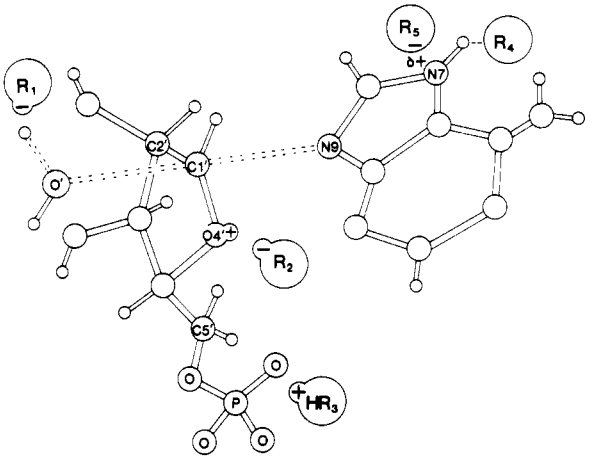

FIGURE 6: Transition state for the AMP nucleosidase reaction. The adenine ring is in the syn configuration, R_1 (pK_a = 6.6) is a proton accepting group, R_2 is an enzyme anion, and R_3 (pK_a = 8.2) is an enzyme cation. The negative charges of the phosphate are not shown. Movement of R_2 is proposed to occur in response to the allosteric activator. Group R_4 (pK_a = 8.2) is protonated in free enzyme and transfers its proton to N7. Group R_5 is proposed to form an ion bridge with R_4H^+ in the free enzyme and to stabilize the charge at N7 in the transition state. Protonation of N7 occurs prior to transition-state formation, since $^{2}H_2O$ kinetic isotopes are near unity.[3]

($R_4H^+ + N7^{\delta-} \rightleftarrows R_4 + N7^{\delta+}$). Two other negatively charged groups, indicated as R_2 and R_5, are proposed to act in transition-state stabilization but do not undergo ionization. These are proposed to have pK_a values too low to appear in the pH profiles for V_{max}/K_m (i.e., less than 4.8). Group R_2 stabilizes the developing carboxonium and influences the fraction of ribosyl hyperconjugation that resides in C1′–O4′ relative to C1′–C2′. Group R_5 is proposed to stabilize the partial positive charge at N7 to reduce the imidazole contribution to the bond order at N9. Other interactions that are not shown in Figure 6 include hydrogen bonding or other interactions to the amino group at C6, since IMP reacts only at 7×10^{-6} of the rate for AMP.[3]

The enzyme-stabilized transition-state structures with and without MgATP differ in the progress in C1′–N9 bond breaking and in the structure of the carbocation. Stabilizing the oxycarbonium with group $^{-}R_2$ can account for both of these effects. The effect of allosteric activation on transition-state structure can be explained most simply by moving $^{-}R_2$ closer to O4′ in the transition state. Stabilization of the oxycarbonium permits an earlier transition state and thus lowers the energy of activation. The magnitude of these effects is small, a change of 0.05 bond order, and thus may reflect only part of the change induced by allosteric activation. For example, electron-inductive effects that make adenine a better leaving group can be isotopically silent, while having a significant effect on the turnover rate. An example of this effect is the V_{max}-deficient mutant of AMP nucleosidase which retains the ability to be activated by MgATP but gives the same ^{3}H1′ and ^{14}C1′ kinetic isotope effects in the presence and absence of MgATP (Parkin & Schramm, 1984). Both transition-state and inductive effects may therefore be involved in the increased V_{max} with allosteric activation. The binding site for MgATP is >20 Å from the catalytic sites (DeWolf et al., 1980); thus these changes are mediated through alterations in protein conformation.

Alternative Transition-State Structures for AMP Nucleosidase. The transition-state structures in Figure 5 are con-

[3] Unpublished observations.

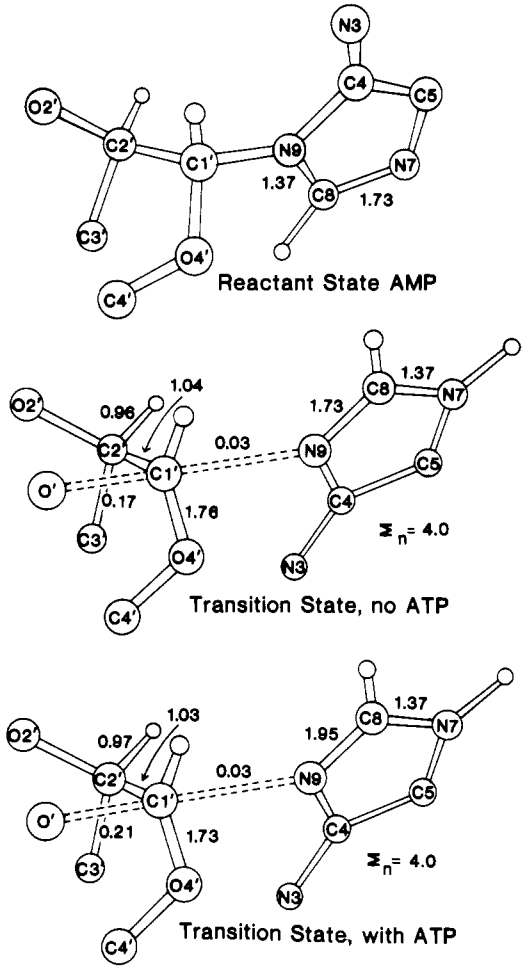

FIGURE 7: Alternative transition-state structures for AMP nucleosidase catalyzed hydrolysis of AMP. The structure labeled "Reactant State AMP" is the solution structure of AMP with N7 unprotonated. Bond orders for N9–C8 and C8–N7 were calculated from the X-ray crystal structure of AMP and Pauling's rule as described under Methods. The structure labeled "Transition State, no ATP" gives the bond orders needed to give agreement between calculated and observed kinetic isotope effects for the enzyme in the absence of allosteric activator. The $\sum_n = 4.0$ indicates total bond order to C1′ in the transition state. Bond order O′–C1′ is 0.17. Protonation of N7 alters the bond distribution in N9–C8 and C8–N7. The structure labeled "Transition State, with ATP" differs from the above structure by increased bond order to the water nucleophile (O′–C1′ bond order = 0.21) and increased N9–C8 bond order. As indicated under Discussion, the source of this increased bond order is not apparent; thus the structures of Figure 5 are favored.

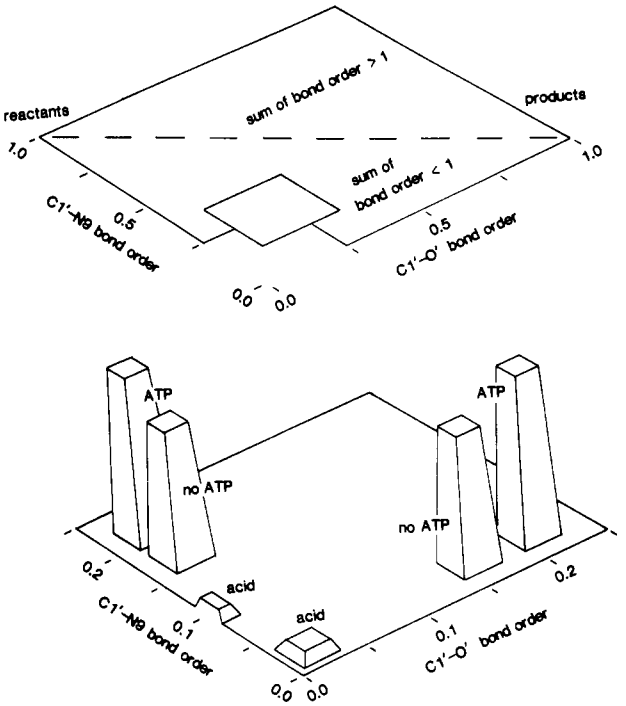

FIGURE 8: Transition-state diagram showing calculated transition-state structures for AMP hydrolysis. Any line connecting the leftmost or reactant corner of the upper figure with the rightmost or product corner represents a possible reaction coordinate for AMP hydrolysis. A single point on a given line represents a two-dimensional transition-state structure with the planar coordinates defining the C1′–N9 and C1′–O′ bond orders. The dotted line connecting reactants and products defines a reaction coordinate in which C1′–O′ bond forming is synchronous with C1′–N9 bond breaking. Each point below the dotted line represents a structure where bond forming lags behind bond breaking. A reaction coordinate defined by restricting the C1′–O′ bond order to 0 describes the S_N1 formation of a carbocation intermediate, represented by the lowest corner of the figure with C1′–N9 and C1′–O bond orders of 0. The lower figure, an enlarged portion of the upper plane, shows the locations of transition-state structures that yield calculated isotope effects consistent with measured isotope effects for the indicated catalysts. The figure indicates the considerable carbocation character found in each transition-state structure and the inverted bond order relationship of the two families of enzymatic transition-state structures. The elevation of each transition-state region approximates the logarithm of the apparent rate constant.

sistent with the kinetic isotope effects and other studies of the enzyme. However, this is not a unique solution. The symmetry of the O′–C1′–N9 reaction coordinate makes assignment of bond order to O′–C1′ and C1′–N9 difficult although the sum of these bond orders is well determined. The transition-state structures in Figure 7 also agree with the kinetic isotope effects. These structures have the O′–C1′ and C1′–N9 bond orders reversed from those of Figure 5. Other changes in transition-state structures that are required to account for the results include an increase in O′–C1′ bond order in the presence of allosteric activator and an increase in N9–C8 bond order to 1.95 compared to 1.73 in the absence of ATP. The transition-state structures of Figure 7 are considered to be less likely than those of Figure 5 because of the high N9–C8 bond order with ATP and the need to invoke changes in bond polarizing forces at both the carboxonium and the adenine ring as well as changes in the relative location of the water molecule. By contrast, the change in transition states induced by allosteric activator in Figure 5 requires movement of only the group that stabilizes the oxycarbonium. It must be emphasized that the experimental data do not permit resolution of these structures. Solvent ^{18}O isotope effects could resolve the problem; however, these are not yet technically feasible for AMP nucleosidase.

General Considerations on Proposed Transition-State Structures. Calculation of a large number of potential transition-state structures for AMP nucleosidase has led only to the structures of Figures 5 and 7. Although the conclusions are not absolute, it is important to emphasize that the possible transition-state structures are confined to small regions of the reaction coordinate space, and one is more likely than the other based on bonding considerations and economy of motion in the allosteric transition. The possible transition states for acid- and enzyme-catalyzed hydrolysis of AMP are indicated in Figure 8, with boundaries corresponding to the error limits of the data. The peak heights represent efficiency of the indicated catalysts in lowering the energy of activation.

Conclusions. Multiple kinetic isotope effects and transition-state calculations have provided transition-state structures for AMP glycoside hydrolysis. Acid-catalyzed hydrolysis occurs from a transition state with protonated adenine as the leaving group and bond orders of only 0.02 to the incoming

H_2O nucleophile and departing adenine. Considering the kinetic restraints on carboxonium ion formation (Jencks, 1980), this transition state is likely to be expanded S_N2-like with definite oxycarbonium character.

The enzymatic reaction stabilizes transition states that are early in the reaction coordinate relative to those stabilized in acid catalysis. Interaction of AMP with the enzyme strains the glycosidic bond, causes protonation of adenine to make it a better leaving group, stabilizes the oxycarbonium, and provides an enzyme-bound water nucleophile for preassociation with the developing oxycarbonium. With the exception of the changes in glycosyl torsion angle, each of the structural changes between reactant and transition states can be quantitated by the family of isotope effects.

Allosteric activation causes the enzyme to stabilize a transition state that is slightly earlier in the reaction coordinate than that in the absence of the allosteric transition. A change in the location of a group that stabilizes the oxycarbonium readily explains this result. The ionizable groups seen in pH profiles of V_{max}/K_m are consistent with the mechanism from isotope effect results. Although the allosteric interaction causes a change in the transition state, the involvement of other, isotopically silent changes cannot be excluded.

An alternative transition-state structure for enzyme-catalyzed hydrolysis proposes a transition-state structure that is late in the reaction coordinate relative to that for acid catalysis. Allosteric activation requires changes in degree of water participation in the transition state, changes in bonding in the adenine ring, and changes to stabilize the oxycarbonium, all of which have no effect on the C1′–N9 bond order. These transition states are considered to be less likely than those discussed above.

Acknowledgments

We thank Dr. Richard Schowen for valuable discussions during the course of this work and Dr. William P. Jencks for his insightful comments on the manuscript. We also thank Shirl A. Collins for her expert typing.

Registry No. AMP, 61-19-8; MgATP, 1476-84-2; AMP nucleosidase, 9025-45-0.

References

Bennet, A. J., Sinnott, M. L., & Wijesundera, W. S. S. (1985) *J. Chem. Soc., Perkin Trans. 2*, 1233–1236.

Burton, G. W., Sims, L. B., & McLennan, D. J. (1977a) *J. Chem. Soc., Perkin Trans. 2*, 1847–1853.

Burton, G. W., Sims, L. B., & Lennan, D. J. (1977b) *J. Chem. Soc., Perkin Trans. 2*, 1763–1770.

Burton, G. W., Sims, L. B., Wilson, J. C., & Fry, A. (1977c) *J. Am. Chem. Soc. 99*, 3371–3379.

DeWolf, W. E., Jr., Fullin, F. A., & Schramm, V. L. (1979) *J. Biol. Chem. 254*, 10868–10875.

DeWolf, W. E., Jr., Markham, G. D., & Schramm, V. L. (1980) *J. Biol. Chem. 255*, 8210–8215.

DeWolf, W. E., Jr., Emig, F. A., & Schramm, V. L. (1986) *Biochemistry 25*, 4132–4140.

Fry, A., & Sims, L. B. (1974) *Quantum Chemistry Program Exchange*, Spec. Publ. No. 1, Indiana University, Bloomington, IN.

Garrett, E. R., & Mehta, P. J. (1972) *J. Am. Chem. Soc. 94*, 8532–8541.

Hermes, J. D., Morrical, S. W., O'Leary, M. H., & Cleland, W. W. (1984) *Biochemistry 23*, 5479–5488.

Jencks, W. P. (1980) *Acc. Chem. Res. 13*, 161–169.

Kraut, J., & Jensen, L. H. (1963) *Acta Crystallogr. 16*, 79–88.

Melander, L., & Saunders, W. H. (1980) *Reaction Rates of Isotopic Molecules*, Wiley, New York.

O'Leary, M. H. (1977) in *Isotope Effects on Enzyme-Catalyzed Reactions*, pp 233–251, University Park Press, Baltimore.

Parkin, D. W., & Schramm, V. L. (1984) *J. Biol. Chem. 259*, 9418–9425.

Parkin, D. W., & Schramm, V. L. (1987) *Biochemistry* (preceding paper in this issue).

Parkin, D. W., Leung, H. B., & Schramm, V. L. (1984) *J. Biol. Chem. 259*, 9411–9417.

Rodgers, J., Femec, D. A., & Schowen, R. L. (1982) *J. Am. Chem. Soc. 104*, 3263–3268.

Romero, R., Stein, R. L., Bull, H. G., & Cordes, E. H. (1978) *J. Am. Chem. Soc. 100*, 7620–7624.

Scharschmidt, M., Fisher, M. A., & Cleland, W. W. (1984) *Biochemistry 23*, 5471–5478.

Schramm, V. L. (1974) *J. Biol. Chem. 249*, 1729–1736.

Sims, L. B., & Lewis, D. E. (1984) *Isot. Org. Chem. 6*, 161–259.

Sims, L. B., Burton, G. W., & Lewis, D. E. (1977) *Quantum Chemistry Program Exchange*, Program No. 337, Indiana University, Bloomington, IN.

Sunko, D. E., Szele, I., & Hehre, W. J. (1977) *J. Am. Chem. Soc. 99*, 5000–5005.

Wilson, E. B., Decius, J. C., & Cross, P. C. (1955) *Molecular Vibrations*, McGraw-Hill, New York.